Particle Reduced, Efficient Gasoline Engines

EUROPEAN COMMISSION
Horizon 2020 | GV-2-2016 | Technologies for low emission light duty powertrains
GA # 723954

Deliverable No.	PaREGEn D1.10	
Deliverable Title	Report on optical diagnostics for fuel-films and mixture inhomogeneities in endoscopically accessed engines. Focus is on implications for combustion strategies	
Deliverable Date	2019-08-31	
Deliverable Type	REPORT	
Dissemination level	Public (PU)	
Written By	Niklas Jüngst (UDE) Muhammad Ali Shahbaz (UDE) Sebastian Kaiser (UDE)	2019-08-19 2019-08-19 2019-08-19
Checked by	Andreas Manz (Bosch)	2019-08-28
Approved by	Simon Edwards (RIC)	2019-08-29
Status	Final	2019-08-30

Publishable Summary

In modern gasoline direct-injection (GDI) engine, soot formation due to inhomogeneities of the fuel/air-mixture in areas around evaporating fuel-films is very likely. Different optical diagnostic techniques have been developed within the PaREGEn project to visualize the different aspects in the particle formation process. These include spray, fuel-film formation and evaporation, combustion, the formation of polycyclic aromatic hydrocarbons and eventually soot.

In the part of the PaREGEn project reported here, some of the developed techniques are applied at Bosch in Renningen, Germany on a thermodynamic, single cylinder direct injection spark ignited (DISI) gasoline engine with small endoscopic optical accesses. Here, the illumination and detection are performed through endoscopes, and the diameter of the ports built in cylinder walls for these endoscopes is 12 mm each. The advantage of thermodynamic engines with small optical accesses over the typical "optical" engines, with quartz liner and quartz piston window, is that the operating range, conditions and heat transfer are similar to real engines. Although the optical diagnostics are typically difficult to apply on such engines, the results represent the actual processes in commercial engines more accurately.

First, fuel-films were visualized on the piston surface using laser-induced fluorescence (LIF). Since the whole piston surface had to be illuminated, flood illumination with laser light at 266 nm was applied by replacing all the lenses in a commercial light-sheet endoscope with a single bi-concave lens. The measurements in this study were performed in a motored engine in skip-fire mode, while the rest-to-work ratio was varied according to the experimental conditions. Two fuels were used: either a commercial gasoline or an iso-octane/toluene mixture with 5 % toluene. Commercial gasoline has many aromatic constituents, which fluoresce when excited with ultra-violet (UV) laser light; while in the iso-octane/toluene mixture, iso-octane served as a non-fluorescent surrogate fuel and toluene acted as a fluorescent tracer. The visualization was performed at different crank angles in each cycle. The survival times for the fuel-film under different conditions were determined. The conditions investigated in this work are: different start of injection times (SOI), different injection pressures (P_{inj}) and different engine temperatures (T_{eng}) to represent cold-start (303 K), transient (328 K) and steady state operation (353 K). Since the commercial gasoline had a variety of fluorescent components, the fluorescence spectra was broad and yielded a higher signal-to-noise ratio as compared to the iso-octane/toluene. The results showed that gasoline had generally 10 times higher fuel-film survival times under all conditions. Also, the fuel-film survival time reduced with later SOI, higher P_{inj}, and higher T_{eng}.

Later, quasi-simultaneous visualization of fuel-film and soot incandescence was performed. The fuel-films were visualized using LIF as described above, while broadband soot incandescence was visualized 2.1 µs after the fuel-films had been visualized. The fuels used in this study were same gasoline and iso-octane/toluene mixture as in the fuel-film investigations in motored engine. The measurements were performed at three reference engine temperatures, 303 K, 328 K and 353 K, to compare the effect of combustion on the survival times of fuel-films. In order to get a steady combustion, the start of injection (SOI) and the injection duration were varied slightly, as compared to the motored conditions. The results showed that soot formation was initiated primarily in the areas above the fuel-films on the piston surface and the injector tip. Also, by a comparison to results from motored conditions, it was observed that combustion had negligible influence on the survival times of the fuel-films for either fuel. This might stem from the fact that the measurements were performed under skip-fire conditions, and the T_{eng} was continuously regulated, and any local temperature increase due to combustion was dimished before or within the next cycle. However, for an engine temperature of 303 K, the difference in the evaporation duration with and without combustion was larger than for the engine temperature of 353 K. Most

probably, the combustion has a stronger influence on the piston temperature when the piston is under cold conditions

Lastly, high-speed colour combustion-visualization of the light scattered by the spray, chemiluminescence and soot incandescence was performed. For illumination, the laser was replaced by a broadband light source. The imaging was performed at 1 °CA resolution. The spray visualization revealed the development of the spray. High-speed visualization of the combustion showed that chemiluminescence and soot formation are temporally separated, as also previously demonstrated in an optically accessible wind tunnel at the University of Duisburg-Essen (UDE). The soot formation was observed to start 20 to 25° crank angle (CA) after the chemiluminescence. The soot formation was observed to be above the fuel-film regions on the piston surface.

Under this work, it was found that the fuel-film survival time was reduced by 30 to 50 % by increasing the P_{inj} from 100 bar to 350 bar. Injecting the fuel later in the intake stroke (later SOI) also reduced the fuel-film survival time. This effect was stronger under cold start conditions than at steady state conditions (353 K), with the fuel-film survival time decreasing by between 36 % to 56 % under cold start conditions. Higher T_{eng} also reduced the fuel-film survival time, and showed the strongest impact of the three parameters investigated. The fuel-film survival time reduced by 60% for gasoline and 57% for iso-octane/toluene when T_{eng} increased from 303 K to 328 K. Further reduction of the fuel-film survival time, when operating at 353 K, was not as strong as at 328K, with gasoline survival time reducing by 42 % while iso-octane survival time remained the same as at 328 K.

Contents

Figures

Tables

1 Introduction

In gasoline direct-injection spark-ignition (DISI) engines, liquid fuel may adhere to surfaces within the combustion chamber generating mixture inhomogeneities and, eventually, soot. To investigate the impact of evaporating fuel-films in combustion as a source of soot formation, instantaneous two-dimensional detection of fuel-films and soot within the combustion chamber is desirable. Laser-based detection techniques are promising to investigate the sub-processes in soot formation non-intrusively.

The correlation between the fuel-films on the piston and the engine-out soot emissions was investigated by Warey et al.[1], Drake et al. [2], Ortmann et al. [3] and Stevens et al. [4]. Warey et al. measured particulate mass and size distributions stemming from piston fuel-films for different fuels [1]. Drake et al. imaged the thickness of evaporating fuel-films by refractive index matching (RIM) and identified pool fires above those by high-speed imaging of the combustion incandescence in an optically accessible DISI engine [2]. They found first soot formation from fuel-rich pockets soon after the spark. However, most of this soot was oxidized in the cylinder during the remainder of the cycle. In contrast, soot formed in pool fires was not oxidized completely, due to low turbulent mixing rates and low temperatures close to the walls, and was detected in some cycles until exhaust valve opening. By simultaneously imaging OH* chemiluminescence (CL) and laser-induced incandescence (LII) of soot, Stojkovic et al. [5] also revealed two distinct stages of soot formation in a DISI engine operating with a stratified fuel/air-mixture. They found that early soot originates from regions with partially premixed combustion close to the spark plug, indicated by OH*-CL, and is oxidized later due to high temperatures (2000 - 2400 K) and turbulent mixing. Soot formation from pool fires occurs later and becomes significant when 80% of the heat has already been released. Temperatures then are much lower (about 1700 K), such that oxidation is unlikely, causing persistent soot and engine-out emissions. In a wall-guided gasoline direct injection (GDI) engine, Ortmann et al. visualized the formation of fuel-films and measured the engine-out emissions of soot and unburned hydrocarbons [3]. Stevens et al. used laser-induced fluorescence (LIF) to show that for late injection, where the piston is close to the injector, significant amounts of fuel impinge on the piston [4]. High-speed imaging of the flame incandescence revealed that under these conditions pool fires may exist into the exhaust stroke because there is not enough time for film evaporation. When fuel-films persist into the exhaust stroke and the local temperature is too low to cause soot formation, unburned hydrocarbons are emitted [6-9]. Recently, Schulz et al. investigated the effect of rail and ambient pressure on the evaporation duration of iso-octane fuel-films in a pressure vessel by high-speed visualization [10]. They found for a vessel temperature of 353 K, a vessel pressure of 1 bar, and a nozzle-wall distance of 45 mm the fuel-film evaporation time to reduce from 0.7 ms to 0.5 ms when increasing the injection pressure from 150 to 300 bar. Although, the mass-transfer and heat-transfer coefficients increase with increasing ambient pressure, the evaporation duration also increases. This is due to the increasing partial pressure of iso-octane and the resulting decreasing concentration gradient between the liquid film's surface (saturation vapour pressure) and the core in the gas phase.

Within the scope of this project, previous work on evaporating fuel-films and soot formation was done in a wind tunnel with an optically accessible test section at UDE [11] (D 1.6). The experimental test section provided large optical access, although it is operated under ambient pressure. Investigations on liquid film formation and evaporation were also done in an optically accessible engine at BOSCH [12] (D1.2). The results have shown that fuel-films evaporate faster in the optical engine than in the wind tunnel. The higher pressure induces a stronger convective heat and mass transfer between the gas phase and the liquid films. Under high pressure, the gas density increases. Therefore, the Prandtl and Schmidt numbers increase which relates to an increase the heat and mass transfer coefficients. The latter is reflected in increased convective heat transfer between the gas phase and the liquid film in an engine, operating at

high pressure. However, in the flow facility at UDE, it was shown that the combustion and hence the convective heat transfer have no influence on the evaporation rate of the liquid films. Therefore, most probably, the convective mass transfer accelerates the evaporation in the optical engine compared to the wind tunnel facility. From a heat-transfer model that was developed at UDE, it is known that the fuel-film temperature adapts to the wall temperature within a few milliseconds after the end of injection. Also from this model, it is known that the evaporative cooling of the liquid film is compensated by the conductive heat flux from the wall.

In the work reported here, the evaporation of fuel-films from the piston surface is investigated in a thermodynamic engine with endoscopic optical access and an aluminium piston. The advantage of this type of engine is that measurements can be taken over the full operating range of a passenger-car engine, and the conditions for heat transfer are comparable to a passenger-car engine. An aluminium piston has higher heat capacity and thermal conductivity than one with quartz, promoting a greater heat flux from the wall to the liquid. During fired operation, the aluminium piston surface is expected to heat up more slowly due to the higher heat capacity compared to quartz. This would result in a lower wall temperature and hence fuel-film temperature compared to the wind tunnel and the optically accessible engine. Therefore, there are two opposing effects on the fuel-film evaporation characteristics when using an aluminium piston instead of quartz.

The suitability of ultra-violet (UV)-transparent excitation and detection endoscopes for the work reported here was tested in advance in the facilities of UDE, before transferring the endoscopes to the thermodynamic engine at BOSCH. The endoscope system is already used in different laser-based measurements for combustion and temperature imaging in the thermodynamic engine at UDE [13, 14]. The diagnostics techniques from sub-tasks 1.3.1 and 1.3.3 of the PaREGEn project, fuel-film imaging with LIF and combustion imaging by natural incandescence, were transferred to the thermodynamic engine.

This report provides results on fuel-film, soot and high-speed colour-combustion imaging in an endoscopically accessible engine carried out together with BOSCH. Results from this report show the evolution and evaporation of liquid films, the spatial and temporal distribution of soot within the combustion chamber, and the evolution of the spray and the flame front in a thermodynamic engine. The information gathered here is used as validation data for sub-models of spray and wall-films in the thermodynamic engine in Sub-task 1.4.2. The operating conditions for the experiments correspond to the operating conditions that were used in the optical engine.

The second chapter describes the specifications of the engine and the endoscopic accesses. In addition, the chapter shows the operating conditions for the experiments as well as the optical layout of the experiments. In the first part of the results, laser-induced fluorescence (LIF) was used to visualize fuel-films endoscopically and to measure their evaporation time (survival time). LIF also shows contributions from gas-phase fuel, forming mixture inhomogeneities. In a second step, fuel-films were visualized simultaneously with natural soot incandescence, giving insights on the instantaneous spatial correlation between evaporating fuel-films and soot. In the third part, results on high-speed real-colour combustion-imaging are presented, showing the spray, the flame front and soot.

2 Methods

2.1 Engine

The experiments were performed at BOSCH in Renningen in a single-cylinder spark-ignited engine, which has a total displacement of 449 cm^3. The engine has a bore/stroke of 82/85 mm and a compression ratio of 12:1 The engine can be operated in either direct injection or port fuel injection mode. Optical access is provided by two small, mutually perpendicular ports with Ø 12 mm each. One is for illumination endoscope and the other is for detection endoscope. The illumination side consists of a housing with a press-fit sapphire window: a Ø 8 mm light-sheet endoscope can be inserted in the housing. The detection endoscope was a commercially available large-aperture UV endoscope from LaVision.

The engine had water-based temperature control, which was used to maintain the required engine temperature (T_{eng}) before starting an experiment and during the experiment. The airflow start of injection (SOI), injection pressure (P_{inj}) and ignition timing were fully controllable. The experiments were performed under either motored or fired conditions. For both conditions, the engine was operated in rest-and-work mode. The rest-to-work ratio (R/W) was varied depending on the fuel and operating conditions, and it was ensured before starting the actual measurements that the fuel-films were completely evaporated before the next work cycle. For gasoline at 303 K engine temperature, a R/W of 39/1 was chosen (i.e., every 40^{th} cycle was a work cycle), whereas for iso-octane/toluene at 353 K engine temperature, a R/W of 9/1 was chosen. For each case, the total number of images taken was chosen to ensure that at least 9 (in some cases 10) cycles are captured.

2.2 Operating conditions

The measurements were performed at 1200 min^{-1} engine speed in the motored and the fired modes. Two different fuels were used in this work, a commercial gasoline fuel and an iso-octane/toluene mixture with 5 % toluene by volume. In this work, 0 °CA is taken to be compression top-dead centre, i.e., crank angles during intake and compression are negative, and one cycle is from -360 °CA to +360 °CA. Measurements were performed at different SOI: 360 °CA, 340 °CA and 320 °CA. The range of SOI was chosen to be able to compare the results with results from the optical engine, where similar SOI were chosen [15]. Also, the endoscopic access on the detection side allows visualization only until 60 °CA. We call this an SOI scan in following text. For an SOI scan, the P_{inj} was kept at 100 bar. Further parameter variations were P_{inj} and T_{eng} (P_{inj} and T_{eng} scans). A P_{inj} scan was performed at 100, 200 and 350 bar, while a Teng scan was performed at: 303 K (30 °C) to represent cold start conditions, 328 K (55 °C) to represent transient conditions and a short trip mode, and 353 K (80 °C) to represent steady state and long trip modes. The maximum engine temperature of 353 K was chosen to make the results comparable to the results from the wind tunnel (D 1.6) where the highest wall temperature was 352 K. In the wind tunnel, the fuel films survived for about 100 ms. The operating conditions are summarized in Table 1. To ensure that same amount of fuel is injected at each P_{inj}, the injection duration was set to 1.70 ms, 1.23 ms and 0.95 ms at 100, 200 and 350 bar, respectively.

Table 1: Operating conditions for fuel-film visualization.

	SOI scan				
	Teng. [K]	**303 K**	**328 K**	**353 K**	**Constants**
Scan	SOI [°CA]	-360		-360	Pinj = 100 bar
		-340		-340	
		-320		-320	
	Pinj scan				
	Pinj [bar]	100		100	SOI = 360 °CA
		200		200	Teng= 303 K und
		350		350	353 K
	Teng scan				
	SOI [°CA]	-360	-360	-360	Pinj = 100 bar SOI = 360 °CA

Table 2 shows the indicated mean effective pressures for the measurements of simultaneous visualization of fuel films and soot, presented in Section 3.1.4.

Table 2: Indicated mean effective pressure for measurements of simultaneous visualization of fuel films and soot.

Indicated mean effective pressure (IMEP) [bar]		
	Gasoline	**Iso-octane**
Teng. = 303 K	2.3	4.5
Teng. = 328 K	2.5	4.04
Teng. = 353 K	3	2.8

2.3 Optical layout

2.3.1 Fuel-film visualization

The optical layout for fuel-film visualization is shown schematically in the Figure 1. The beam of a Nd:YAG laser at 266 nm with a maximum repetition rate of 10 Hz was introduced into the cylinder via a laser guiding arm and a laser endoscope. The laser endoscope was modified to produce flood illumination instead of a light sheet by replacing all the lenses with a single bi-concave lens (focal length= -6 mm). The laser energy was ~9 mJ/pulse as measured after the endoscope.

The imaging was performed by UV detection endoscope producing an intermediate image on a field lens. This image is then re-projected onto the camera sensor through a spectral filter and a 100 mm f/2.8 UV lens, without a rigid connection in between. For the iso-octane/toluene mixture, a 292/40 nm bandpass filter was used. Since gasoline had a variety of fluorescent components and a broadband fluorescence specta, a longpass 266 nm filter was used. Both filters blocked scattered laser light. The camera used for fuel-film visualization was an intensified CCD camera from LaVision with a resolution of 1040 × 1376 pixel^2, and a S20 photocathode with a decay time of 0.2 µs. The imaging was performed with 2×2 binning for gasoline and 4×4 binning for iso-octane/toluene mixture. The gate was set at 100 ns, and gain was 50 (as read in the control software DaVis) for gasoline and 60 for the iso-octane/toluene mixture.

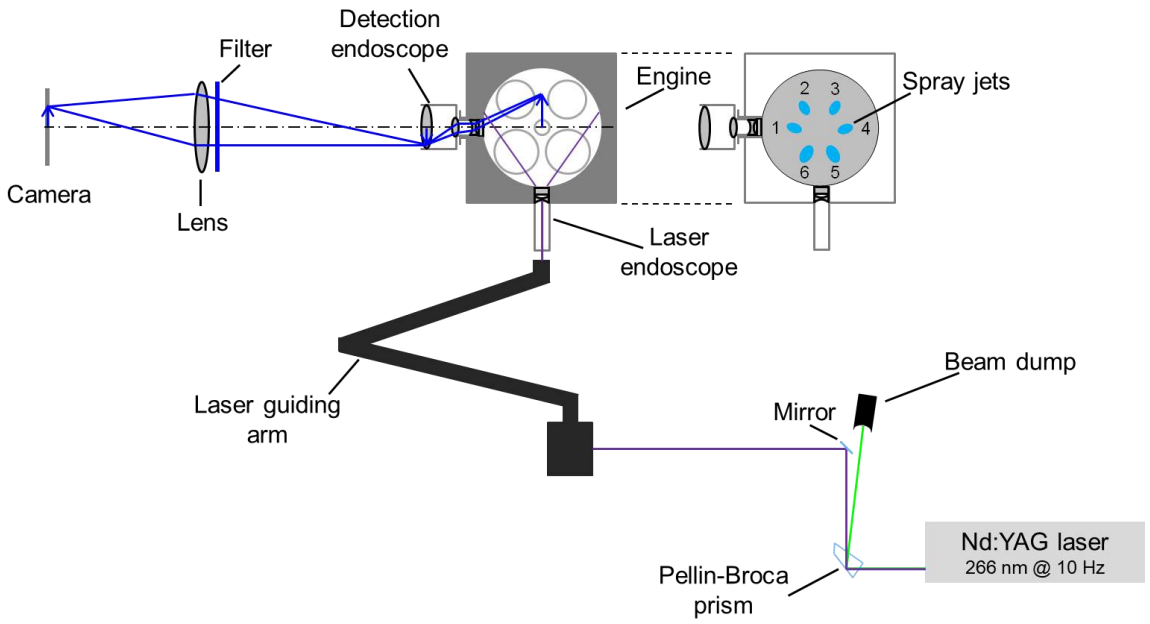

Figure 1: Schematic diagram of the experiment.

2.3.2 Simultaneous fuel-film and soot visualization

For the simultaneous visualization of fuel-films and soot incandescence, an intensified CCD camera with a fast-decay phosphor was employed. This allowed for a double-frame acquisition. The first frame captured the LIF of fuel-films with an exposure time of 100 ns. The second frame captured soot incandescence 2.1 µs after the first frame. The exposure time for the second frame was varied between 5 and 10 µs. The gain was 50 for the first frame and was varied between 30 and 40 for the second frame. An LP 266 filter was used for all simultaneous fuel-film and soot visualization. Simultaneously, an engine exhaust particle sizer (TSI, EEPS spectrometer Model 3090) measured the particle size distributions and total soot-particle number concentrations in the exhaust gas with a sampling rate of 10 Hz.

2.3.3 High-speed colour combustion-imaging

For high-speed colour combustion imaging, the laser illumination was replaced by a broadband halogen-lamp light source from Karl Storz (Technolight 270). The light was introduced into the cylinder by a fibre optic cable and the same flood-illumination endoscope as used in fuel-film visualization. The camera used was Photron FASTCAM SA-Z high-speed colour camera with a maximum repetition rate of 20000 fps at 1024×1024 pixel^2 resolution. For this measurement, the repetition rate was reduced to 7344 fps in order to take images at 1 °CA resolution at 1200 min^{-1} engine speed. Spray visualisation was performed from -360 °CA to -300 °CA, and combustion was visualised from -20 °CA to +60 °CA. The exposure time was set to 134.6 µs for spray visualisation but to only 70 µs for combustion visualization, due to the very high intensity of soot incandescence. The soot incandescence was further reduced by a 1 mm thick BG23 filter in front of the lens. Measures taken to further reduce the soot incandescence would also reduce chemiluminescence signal, which was already much weaker than soot incandescence. Thus, an exposure time of 70 µs was used to ensure minimum chemiluminescence signals, even though the soot incandescence was then too bright at later crank angles and mostly saturated the sensor.

3 Results

3.1 Fuel-film evaporation

3.1.1 Gasoline

Figure 2 shows background-subtracted single-shot images from fuel-film evaporation of gasoline. The images shown were taken at -350 °CA to visualize the spray, as well as the fuel-films in the following cycles. The images were taken in each cycle, images from every 3rd cycle are shown here in Figure 2, after the first two cycles. The engine was operated here at rest-to-work ratio of 39:1, and 400 images were taken. This yielded images from 9 cycles, used to estimate the mean survival time for the fuel-films. The background was obtained by taking the mean of images one cycle before the injected cycle. This strategy was chosen because the piston surface was covered with engine oil, which also fluoresces when excited at 266 nm. The fluorescence of engine oil was observed using long pass 266, as well as band pass 292/40 filters. Also, due to the in-cylinder air movement, the oil distribution was continuously changing, so an in-situ background was a suitable approach.

Under these conditions, the gasoline fuel-film can survive as long as 31 cycles, as shown in Figure 2. The mean survival time of the fuel-film in terms of number of cycles after injection was determined for this as well as all other operating conditions and the results are presented in Sub-section 3.1.3.

3.1.2 Iso-octane/toluene

Figure 3 shows the background-subtracted and averaged images of evaporating iso-octane/toluene fuel-film over one cycle. The fuel was injected at -360 °CA at P_{inj} = 100 bar. The engine temperature was at 353 K, representing the steady state condition. The iso-octane/toluene fuel-film evaporated quickly at these conditions. Therefore, instead of same crank angles in subsequent cycles, averaged images from different crank angles in the work cycle (and few from subsequent cycle) are shown here. Since the signal-to-noise ratio was low in later crank-angles, images at same crank angle from 10 recorded work cycles were averaged and are shown here. The images shown in middle row of Figure 3 also show some gas-phase LIF signals on the upper right side of the images. This is not visible in the first row due to a lesser amount of vaporized iso-octane/toluene and the wider range of the colour-bar. Although the colour-bar range is same for the third row, the vaporized iso-octane/toluene is not visible as the exhaust stroke is in progress and vaporized iso-octane/toluene has already left the cylinder. Figure 3 shows that at this operating point the fuel-film survives only a single cycle. A small residual film is visible on the outer side of the fuel-film at -340 °CA, as marked in Figure 3 in the next cycle. However, it is completely evaporated by -320 °CA.

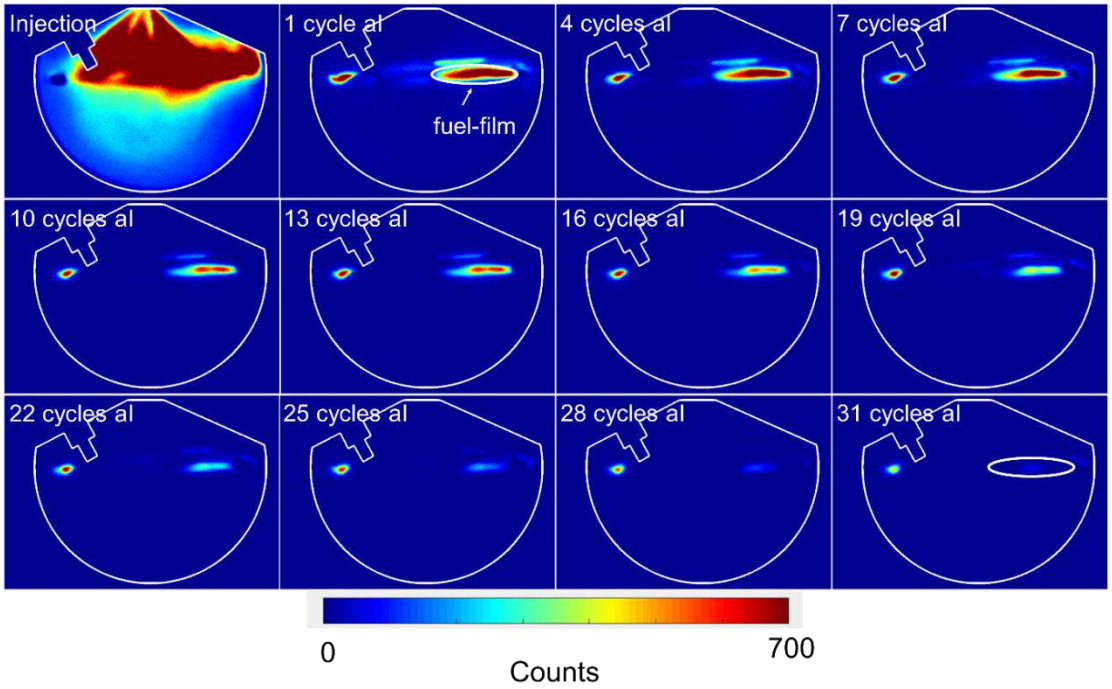

Figure 2: Single-shot images for fuel-film evaporation at T_{eng} = 303 K , SOI = -360 °CA, and P_{inj} = 100 bar. In this example, the fuel-film survives 31 cycles after ignition (aI).

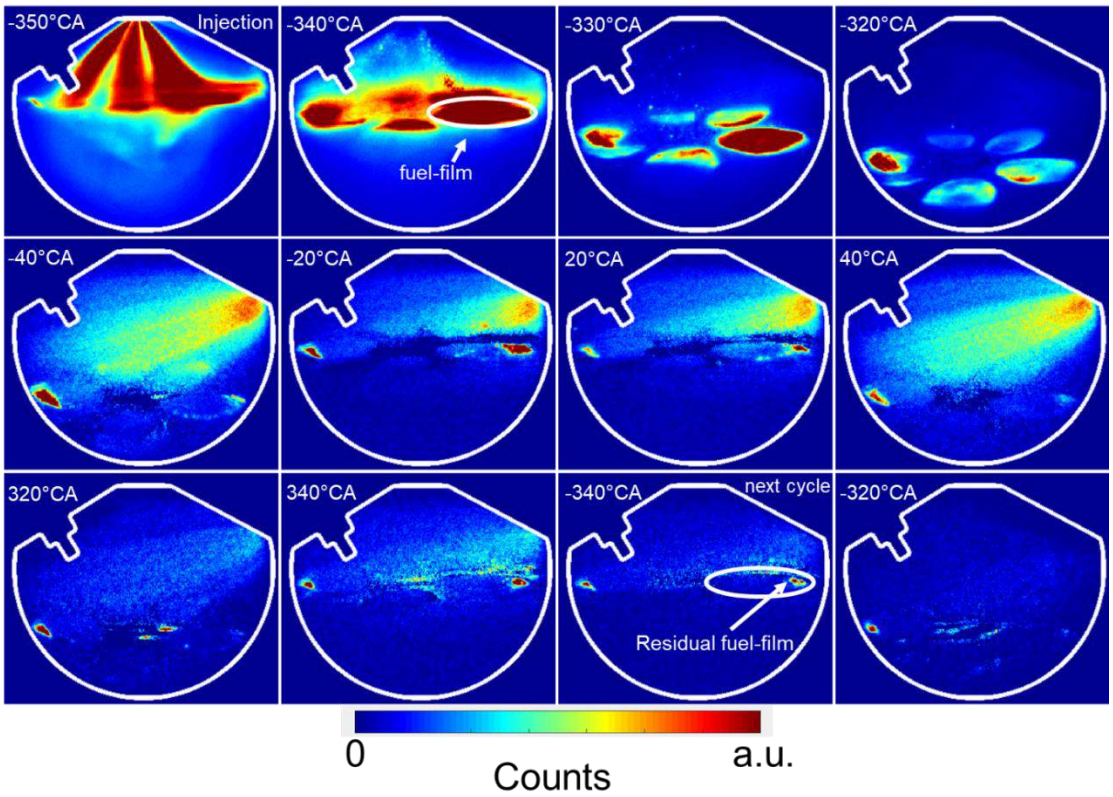

Figure 3: Iso-octane/toluene fuel-film evaporation at 353 K engine temperature, SOI at -360 °CA and P_{inj} of 100 bar. Under these conditions, the fuel-film has survived 1 cycle.

3.1.3 Fuel-film survival time

As mentioned earlier, the engine was operated in skip-fire mode. For each fuel injection, the total number of cycles that the fuel-film survived was noted, and an average value of fuel-film survival time was determined by averaging the number of cycles. A standard deviation for fuel-film survival time was also calculated. In this section, the points on the plots represent the mean survival time for fuel-films, and the error bars represent the standard deviation.

Figure 4 shows the variation of fuel-film survival time with different SOI at different T_{eng} for gasoline. At 303 K, the fuel-film survives up to an average value of 28 cycles. The survival time is reduced to 25 cycles at SOI = -340 °CA, and to 18 cycles at SOI = -320 °CA. This is because at later injection, more fuel evaporates before hitting on the piston surface. This results in less mass of fuel-film on the piston surface, which evaporates faster. However, at 353 K engine temperature, the survival time for SOI = -360 °CA was close to SOI = -320 °CA, with 6.3 and 5.5 cycles respectively. Whereas, the survival time at SOI = -340 °CA was longer with a value of 8.8 cycles. The possible reason for shorter survival time at SOI = -360 °CA is faster evaporation resulting from higher heat flux from hot piston surface to the fuel-film. At SOI = -340 °CA, the survival time is longer than at SOI = -360 °CA due to lower temperature of the fuel-film caused by evaporative cooling. This phenomenon, however, needs some further investigation. At SOI = -320 °CA, the shorter survival time was due to more fuel evaporating before hitting the piston surface.

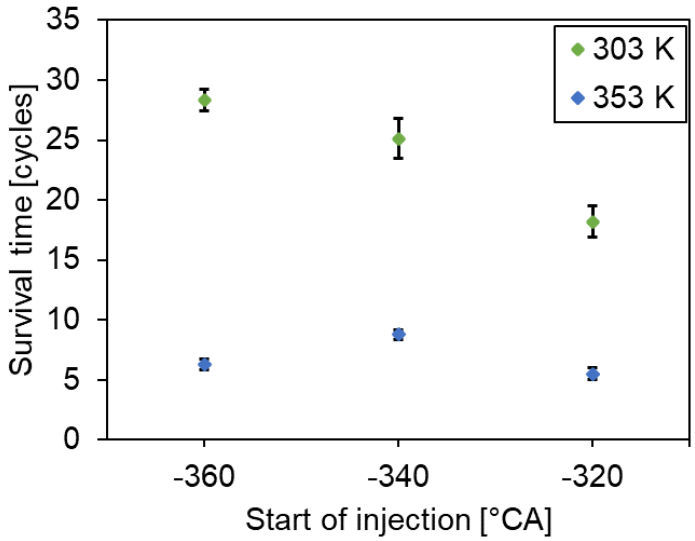

Figure 4: Fuel-film survival time for gasoline with different start of injection timings. P_{inj} = 100 bar.

The fuel-film survival time for gasoline at different P_{inj} is shown in Figure 5. The results at both 303 K and 353 K engine temperature show a reduction in fuel-film survival time with increasing P_{inj}. At T_{eng} = 303 K, the fuel-film survival time is reduced from 28 cycles at 100 bar P_{inj} to 21 cycles at 200 bar, and 14.6 cycles at 350 bar P_{inj}; a reduction by approximately 50 % as compared to P_{inj} = 100 bar. At T_{eng} = 353 K, the average fuel-film survival time is 5.5 cycles at P_{inj} = 100 bar, 4.1 cycles at 200 bar and 3 cycles at 350 bar. At this engine temperature, the fuel-film survival time at P_{inj} 350 bar is again reduced by about 50 % as compared to P_{inj} = 100 bar.

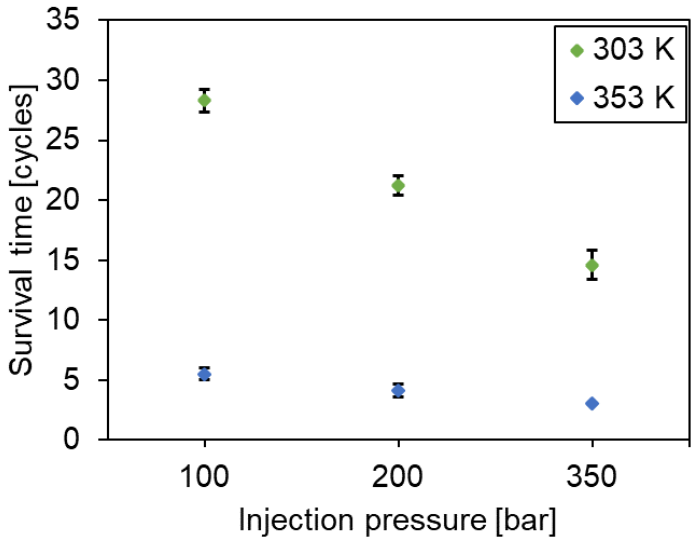

Figure 5: Fuel-film survival time for gasoline with different P_{inj}s. SOI at -360 °CA.

Figure 6 shows the fuel-film survival times with different T_{eng}. 303 K represents a cold start condition, 328 K represents a transient or short-trips-mode condition, and 353 K represents a typical steady-state engine temperature. The fuel was injected at -360 °CA and P_{inj} was 100 bar. The fuel-film survival time is shortened notably from 28 cycles at 303 K engine temperature to 11 cycles at 328 K. At 353 K engine temperature, the survival time was further reduced to an average value of 6.3 cycles.

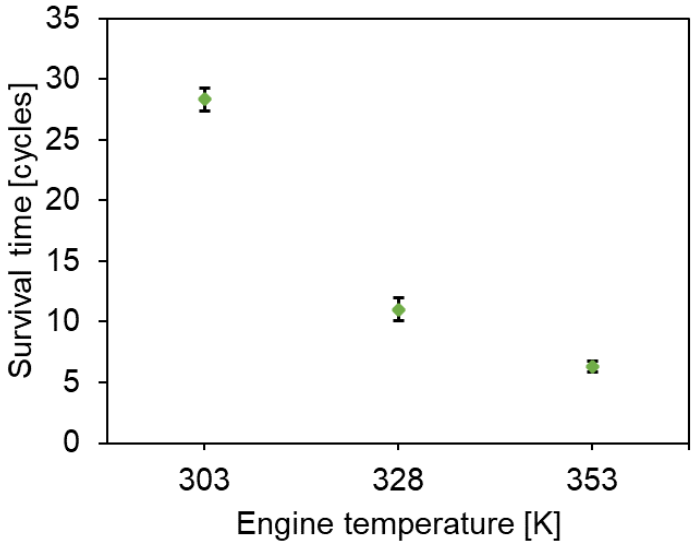

Figure 6: Fuel-film survival time for gasoline with different engine temperatures. SOI = -360 °CA at P_{inj} = 100 bar.

Figure 7 shows the fuel-film survival time for iso-octane/toluene mixture with different SOI at two different engine temperatures. At T_{eng} = 303 K and SOI = -360 °CA, the fuel-film survived for the longest time, an average of 2.3 cycles. This is considerably shorter than survival time of gasoline fuel-film at similar conditions. This is due to heavy hydrocarbons in the gasoline, whereas iso-octane is a single component hydrocarbon with high vapour pressure. The survival time is reduced to 1.9 cycles at SOI at -340 °CA and to 1 cycle at -320 °CA. This, along with the gasoline survival times at similar conditions, suggest that at cold start conditions, the fuel should be injected late during the intake stroke, to significantly reduce the evaporation duration of the fuel films according to Figure 4: Fuel-film survival time for gasoline with

different start of injection timings. P_{inj} = 100 bar.Figure 4. At 353 K T_{eng}, the fuel-film survives for 1 cycle at SOI at -360 °CA, and for half cycle at -340 °CA and -320 °CA. For later two cases, the fuel-film had always completely evaporated by the end of cycle.

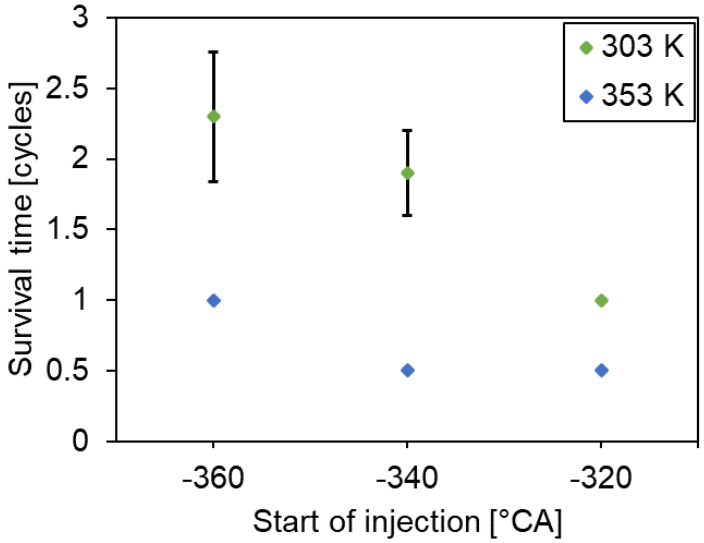

Figure 7: Fuel-film survival time for isooctane/toluene mixture with different start of injection timings. P_{inj} = 100 bar.

Figure 8 shows the variation of fuel-film survival time with different P_{inj} at two T_{eng}. At T_{eng} = 303 K, the fuel-film survives 2.3 cycles at P_{inj} =100 bar, and 2.1 cycles at P_{inj} = 200 bar. The survival time at P_{inj} = 350 bar was 1.6 cycles, which is 70% of the survival time at 100 bar P_{inj}. At T_{eng} = 353 K, the survival time is 1 cycle, 0.5 cycle, and 0.5 cycle for 100, 200, and 350 bar P_{inj} respectively. These values are averaged from 9 cycles and have a standard deviation of zero. At this engine temperature, the survival time at 350 bar is 50% of the survival time at P_{inj} = 100 bar, which is consistent with the results obtained from gasoline fuel-films.

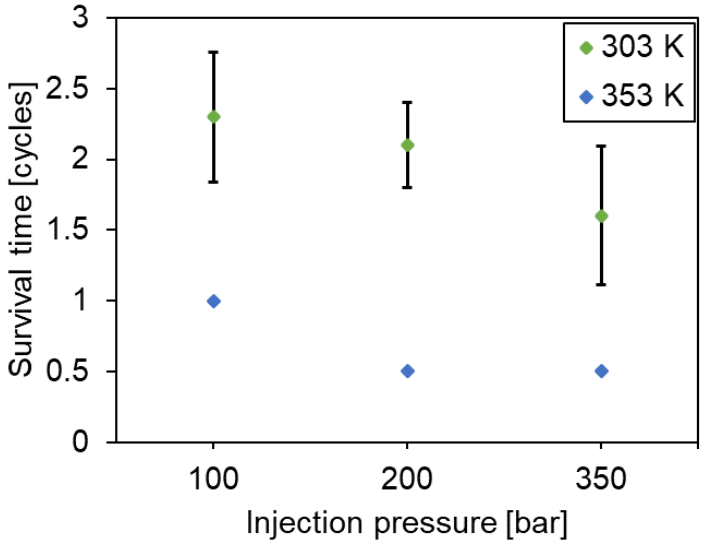

Figure 8: Fuel-film survival time for isooctane/toluene mixture with different P_{inj}s. SOI at -360 °CA.

Figure 9 shows the fuel-film survival time for iso-octane/toluene mixture at different T_{eng}. The fuel was injected at -360 °CA with P_{inj} = 100 bar. The survival time is 2.3 cycles at T_{eng} = 303 K, and 1 cycle for 328 K and 353 K. This result is also consistent with the results from gasoline, where survival time is notably

reduced at T_{eng} = 328 K, and the further reduction at 353 K was not as significant as compared to reduction observed between 303 K and 328 K.

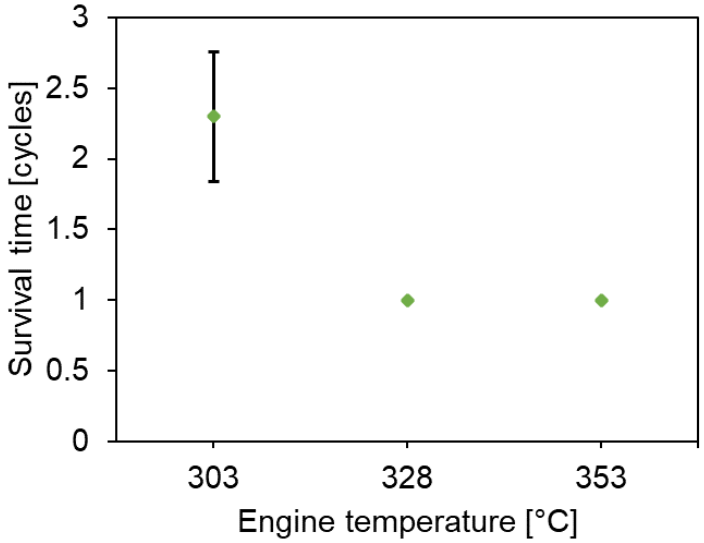

Figure 9: Fuel-film survival time for isooctane/toluene mixture with different engine temperatures. SOI at -360 °CA at 100 bar.

Figure 10 shows the influence of combustion on the survival times of fuel-films of gasoline and the isooctane/toluene mixture. For all the points shown, SOI is at -320 °CA at P_{inj} = 100 bar, except for the measurement with iso-octane/toluene mixture at T_{eng} = 353 K. At this operating point, SOI was -360 °CA to obtain a steady centre of combustion. The corresponding point from motored conditions also had the same SOI. Since no measurements were performed with SOI at -320 °CA at T_{eng} = 328 K under motored conditions, the points at this temperature are only from fired condition to show a trend. The figure shows that there is no significant difference in fuel-film survival times for motored and fired operation at 303 K and 353 K engine temperatures.

The figure shows that there is no significant difference in fuel-film survival times for motored and fired operation at 303 K and 353 K engine temperatures. It is noteworthy here that these investigations were performed under skip-fire mode. Since the T_{eng} was externally regulated, so the local increase in the piston surface temperature was probably dimished before or within the next cycle. In continuous-fire mode, the effect of combustion is present in every cycle and be more significant. This also explains the slightly higher difference in fuel-film survival times with and without combustion at T_{eng} = 303 K, where the effect of combustion is slightly more significant as compared to at T_{eng} = 353 K.

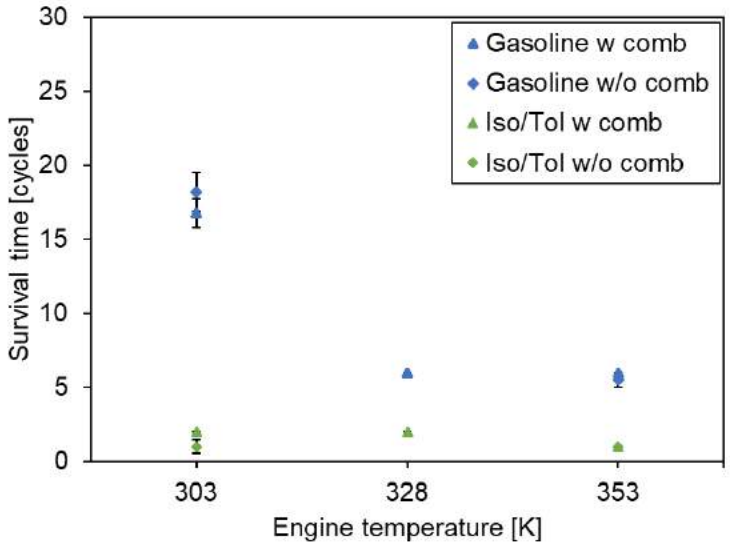

Figure 10: Fuel-film survival time for gasoline and isooctane/toluene mixture in motored and fired operation.

3.1.4 Gasoline

The left two columns of Figure 11 show single shots of natural soot incandescence (red) and fuel-film LIF (turquois). For reproducible combustion events, indicated by a constant indicated mean effective pressure (IMEP), the SOI was set to -320 °CA. The rest to work ratio was 20:1. The two phenomena were imaged quasi-simultaneously, as described in Section 2.3.2. The signals in each image are normalized with respect to the maximum signal intensity. The two left columns in Figure 11: (left) Single shots and (right) mean images of soot incandescence (red) and fuel-films (turquois). The fuel was gasoline and the engine temperature 303 K. show single shots at different crank angles. The corresponding ensemble averages from 10 single shots are shown in the right column. At 20 and 30 °CA only two of the in total six fuel-films are visible due to the inhomogeneous endoscopic laser illumination. These are fuel-films 5 and 6 (spray pattern is shown in D 1.6 and in Figure 1), as indicated in the left single shot at 20 °CA. Small soot pockets are detected near the fuel-films. The image shows natural incandescence throughout the entire combustion chamber, most probably coming from chemiluminescence of the flame front. At 30 and 40 °CA, the detected soot incandescence covers a broader region near film 5. The chemiluminescence extinguished at 30 °CA, as seen in the mean image. Film 1 is visible in the left single shot at 40 °CA. At 50 °CA, also fuel-films 3 and 4 have moved into the laser illumination. At 60 °CA, the illumination visualizes only fuel-films 4 and 5 on the piston surface. At the same time, soot incandescence near the fuel-films has almost completely extinguished while soot incandescence is detected near the injector tip, probably from wetting the tip with fuel during injection.

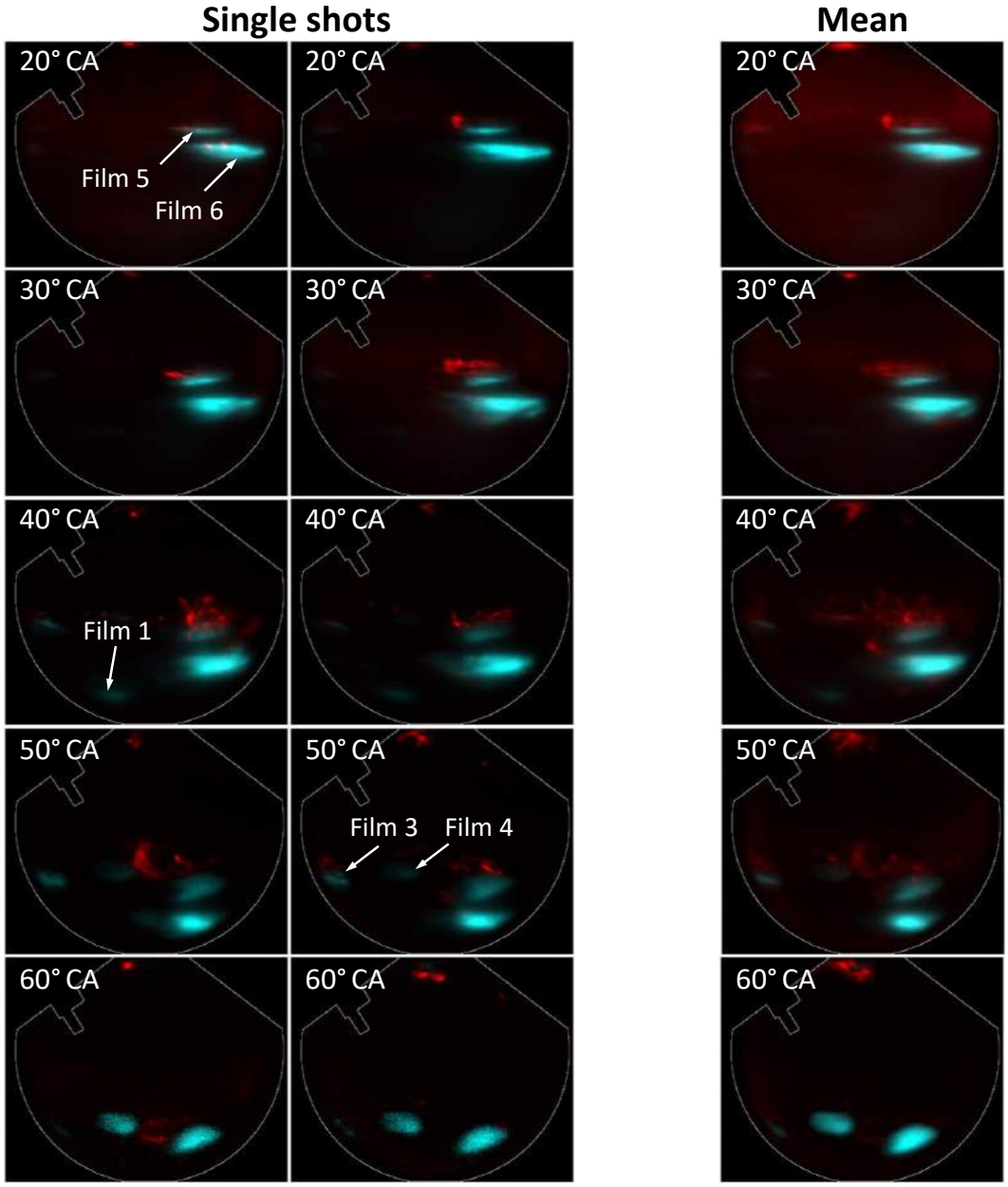

Figure 11: (left) Single shots and (right) mean images of soot incandescence (red) and fuel-films (turquois). The fuel was gasoline and the engine temperature 303 K.

The corresponding images from an elevated T_{eng} of 353 K are shown in Figure 12. Comparing the images with Figure 11 shows that the fuel-films have sharper edges in the high temperature case and a more discrete shape. However, for unknown reasons in these experiments, the piston surface was covered with a lot of engine oil. Therefore, the LIF signal might also stem from oil that significantly contributes to the formation of soot. Here, soot is detected near the fuel-films on the left in broad regions already at 20 °CA. The single shots imply that the flow is moving from right to left along the piston surface, indicated by the extended fuel-film regions towards the left and the structure of the soot incandescence. The fuel-films show a substantially different shape than at an engine temperature of 303 K. They cover a larger area on the piston surface and seem to consist of interspersed thin and thick parts. Soot incandescence is also

detected in regions where no fuel-films are detected. Also at 30 °CA, the single shots imply convective transport of fuel and soot towards the left side of the combustion chamber. In single shots at 40 °CA, the transition region between fuel and soot is clearly visible, indicated as “1” and “2”. Some fuel is lifted from the piston surface, stretches out in the flow and eventually turns into soot while a dark region is located between the two species, as shown at the labels “1” and “2”. The discrete LIF pockets close to the two labels might either stem from liquid fuel droplets, emerging from the film due to the flow, fuel-vapour, or even polycyclic aromatic hydrocarbons (PAH).

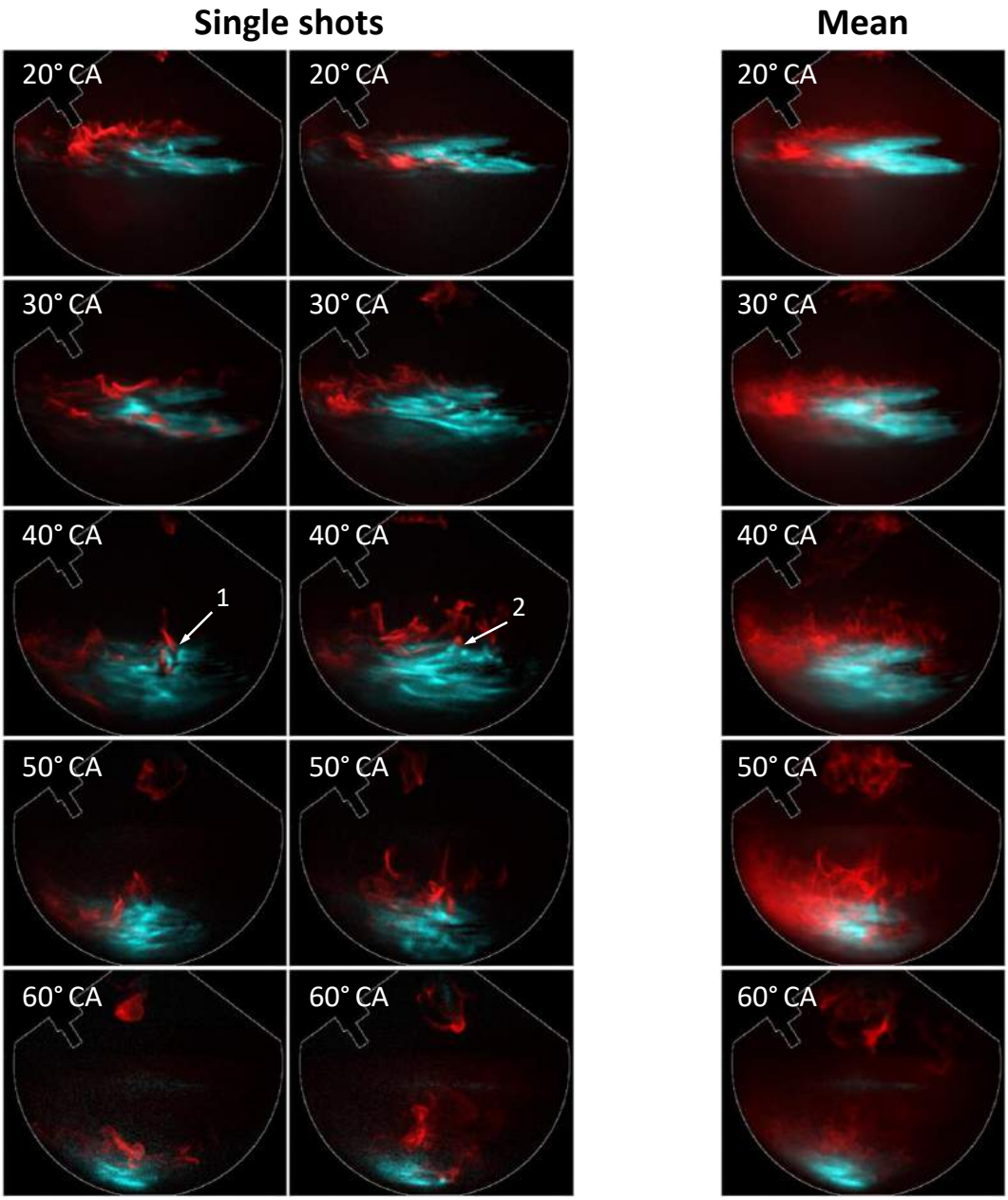

Figure 12: (left) Single shots and (right) mean images of soot incandescence (red) and fuel-films (turquois). The fuel was gasoline and the engine temperature 353 K.

The ensemble-average images of soot incandescence and LIF at 20, 30 and 40 °CA show broad regions of soot incandescence, originating from the fuel-films, and extending far into the left region above the piston

surface. At 50 °CA, the fuel-films substantially reduce in area. This results from the fuel-film evaporation in the right parts and from the increasing inhomogeneous illumination in this region. At 50 °CA the mean image shows that the soot is slightly lifting up from the piston. Apparently, the gas expansion associated with combustion pushes the mixture inhomogeneities towards the piston at 20 and 30 °CA, leading to the formation of soot in a thin layer. At later crank angles, when the flame front has passed, mixture inhomogeneities propagate further away from the piston surface, leading to soot formation in the core region of the combustion chamber, as shown in the single shots at 50 and 60 °CA. At 60 °CA, the soot incandescence becomes less pronounced. In general, it needs to be taken into account that an oil film on the piston leads to the interference of LIF signal from fuel and oil. Also, detected soot incandescence stems from soot originating either from oil or fuel-films. Fuel-film formation and soot incandescence are very similar for the two engine temperatures of 328 and 353 K. Isolated fuel-films are more pronounced at 303 K than at the higher temperatures. In the latter, a broad LIF signal covers the piston surface.

Figure 13 shows the soot-particle number concentrations versus the measurement time for the three different T_{eng}. The number concentration was measured with the engine exhaust particle sizer (EEPS) with 10 Hz, versus the measurement time for the three different engine temperatures. The higher the engine temperature, the more the total concentration scatters over the measurement time. However, for all the cases the mean concentrations remain approximately constant, indicating that there is no effect of the skip firing operation on the soot-particle number concentration. This is because the EEPS blurs out this effect. Surprisingly, the case with the highest engine temperature shows also the highest soot concentration. Here the average number concentration is about $6 \cdot 10^7\ cm^{-3}$ while it is only $2.2 \cdot 10^7\ cm^{-3}$ and $0.5 \cdot 10^7\ cm^{-3}$ for engine temperatures of 328 and 303 K, respectively. The reason for this non-intuitive correlation is that the fuel-films remain on the piston surface for many cycles for lower engine temperatures. While the fuel-films remain on the piston for about 17 cycles for an engine temperature of 303 K, the films have evaporated after about 6 cycles for engine temperatures of 328 and 355 K. Therefore, at a temperature of 303 K much less fuel evaporates from the film into the gas phase and contributes to soot formation in each cycle. Taking into account that in reality fuel-film evaporation occurs in continuously fired operation and assuming that combustion generally does not significantly increase the engine temperature over the evaporation period, the soot-particle number concentration would increase by about the number of cycles over which the films evaporate. Then, the fuel-films would contribute to soot formation in every cycle. Taking the fuel-film survival time from Section 3.1.3 into account results in the soot-particle number concentrations of $3.8 \cdot 10^8\ cm^{-3}$, $1.32 \cdot 10^8\ cm^{-3}$ and $8.5 \cdot 10^7\ cm^{-3}$ for 355, 328 and 303 K engine temperatures, respectively. The fact that the concentration is still about a factor of 4.5 higher for 355 K than for 303 K most probably originates from the oil on the piston surface, which accumulated during the measurements and contributed to soot formation during the measurements. Therefore, the results shown in Figure 13 cannot exclusively be assigned to the soot formation from iso-octane During the different measurements, the engine temperature was successively increased, which lowered the oil's viscosity and most probably enhanced the accumulation on the piston.

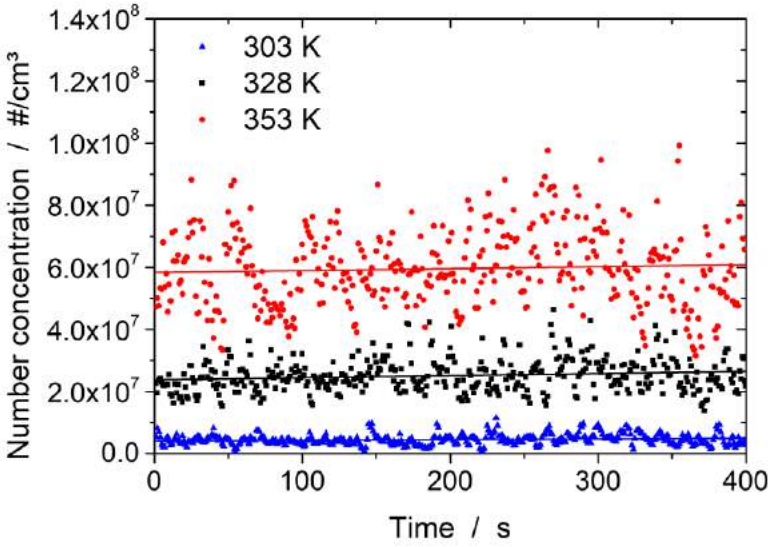

Figure 13: Soot total number concentrations versus the measurement time for three different engine temperatures and gasoline fuel.

Figure 14 shows the soot incandescence integrated across the field of view (which itself represents a line-of-sight integration) in the images from Figure 11 and Figure 12 for the three different engine temperatures. Consistent with the results from the EEPS, the soot incandescence increases with increasing engine temperature. The traces in Figure 14 show an increase in the soot incandescence until about 10 and 20 °CA, while it decreases at later crank angles. This is due to two reasons. First, the soot is cooling down quickly with progress in time, emitting less thermal radiation. Second, the collection efficiency of the imaging system is decreasing when the piston moves down.

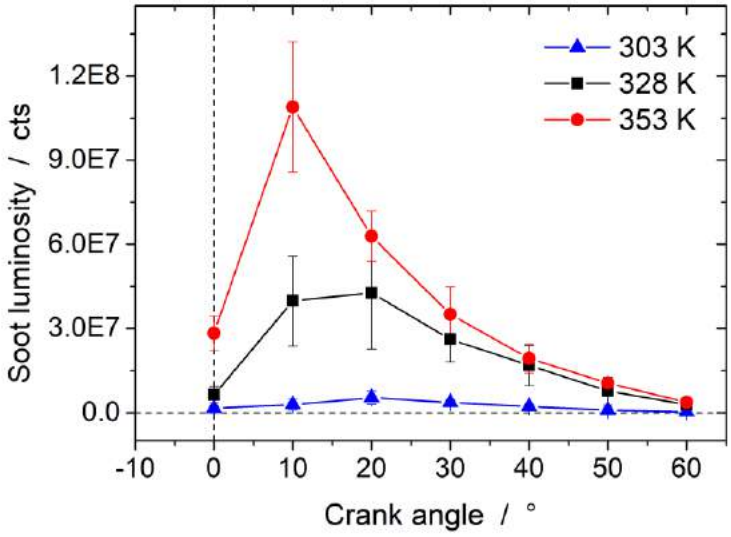

Figure 14: Integrated soot incandescence for three different engine temperatures and gasoline fuel. Error bars indicate the standard deviation over 10 single cycles.

3.1.5 Iso-octane

Results from fuel-film LIF and soot incandescence for iso-octane/toluene are shown in Figure 15. For this engine temperature, 303 K, the SOI was -360 °CA. To clean the piston from oil deposits, the engine was fueled with methane before each measurment until a negegible concentration of soot was measured in the EEPS. Therefore, soot incandescence and measured number concentrations in these experiments can be exclusively assigned to mixture inhomogenities from the iso-octane fuel.

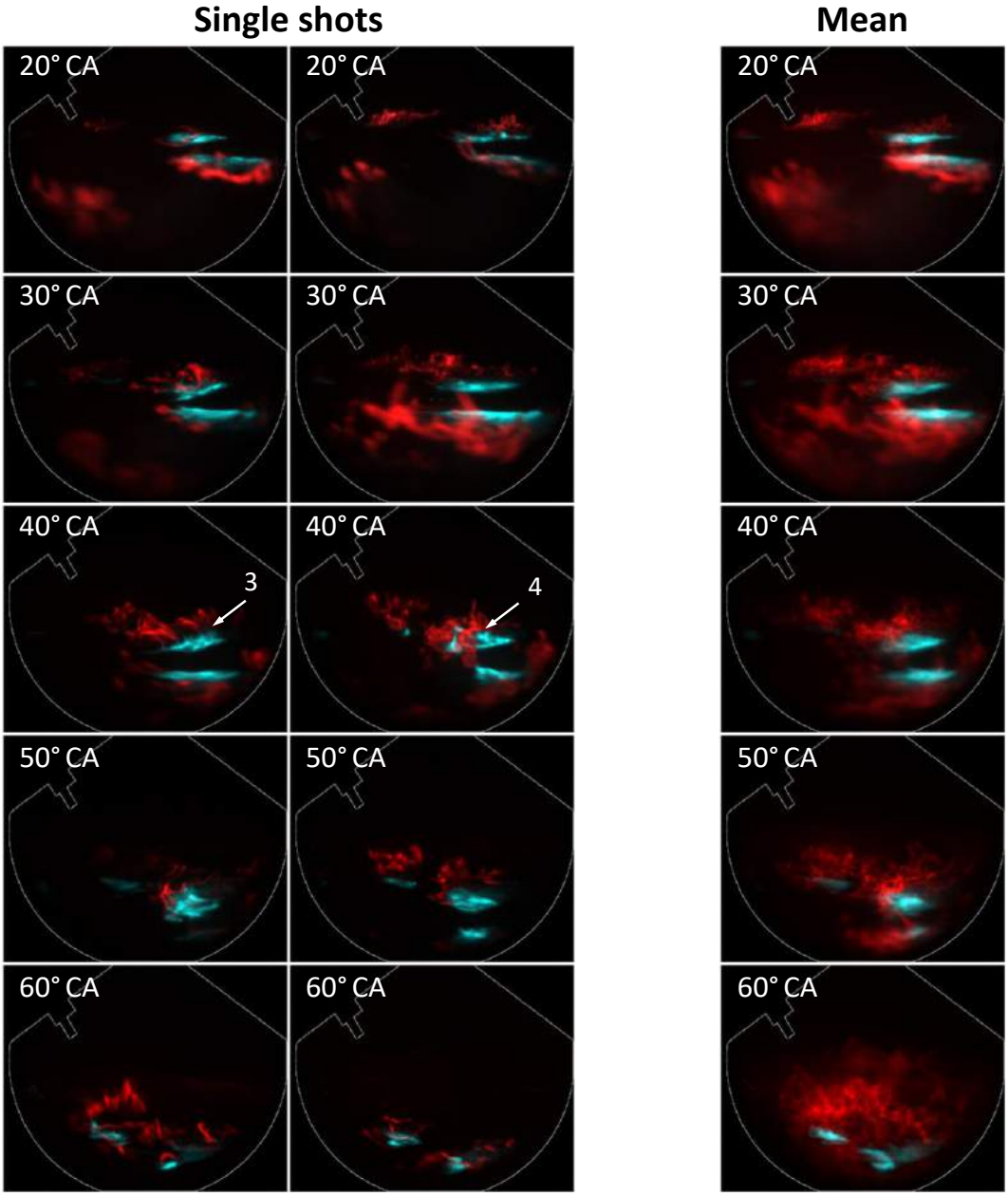

Figure 15: (left) Single shots and (right) mean images of soot incandescence (red) and fuel-films (turquois). The fuel was iso-octane and the engine temperature 303 K.

Compared to gasoline (Figure 11), the iso-octane fuel-films cover a smaller area and show a sharper structure, as shown in Figure 16. While very little soot incandescence was visible at 20 °CA with gasoline, significant soot is found for iso-octane. Most probably, the higher vapour pressure of iso-octane compared to gasoline results in a higher fraction of fuel that has already evaporated at 20 °CA. This in turn results in a locally richer fuel/air-mixture, making the formation of soot more likely. The blurred LIF signal, labeled as “3”, follows the flow and results in the formation of soot. Here, a dark region is found between the LIF signal and the soot incandescence, indicating the nucleation region where fuel turns into soot (D 1.6). Label “4” indicates the spatial overlap of LIF signal and soot incandescence without a transition region in between. At 50 °CA, the convective transport with the flow of fuel and soot is apparent. At 60 °CA, the fuel-films have mostly evaporated.

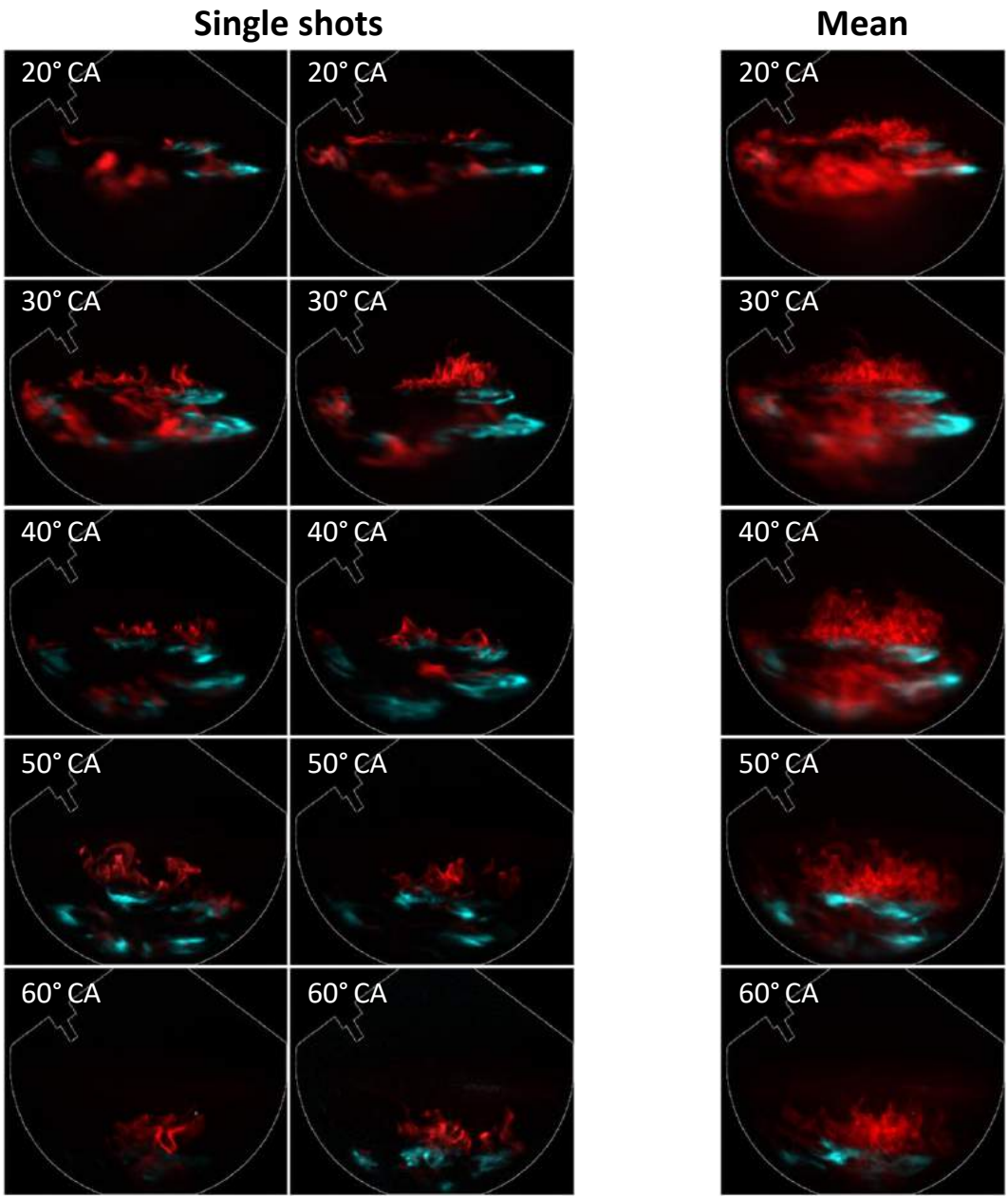

Figure 16: (left) Single shots and (right) mean images of soot incandescence (red) and fuel-films (turquois). The fuel was iso-octane and the engine temperature 353 K.

Figure 16 shows iso-octane fuel-films and soot incandescence for an engine temperature of 353 K. Here, SOI was changed to -320 °CA and the injection time increased to 2.5 ms to achieve a constant IMEP and CA50 throughout the cycles. Compared to the case with a temperature of 303 K at 30 °CA, the fuel-films show more structure and regions of high intensity in the outer part of the wetted area. Most probably, the decreased viscosity of the fuel at elevated temperature enhances the accumulation into thick regions on the piston surface. Again, significant soot incandescence is found at already 20 °CA. At 20 and 30 °CA soot incandescence is found near all the fuel-films. At 40 and 50 °CA the direction of the flow is not from right to left anymore so that soot incandescence is now found very close to the fuel-films with some transition region in between. In contrast to the cases with 303 K, additionally fuel-films 1, 2, 3 and 4 are visible.

Figure 17 shows the total soot concentrations, measured in the EEPS, for the three engine temperatures 303, 328 and 353 K. Again, the case with the lowest temperature shows the lowest concentration of $0.5 \cdot 10^7\ cm^{-3}$, which is similar to the case with gasoline. The soot number concentration increases with increasing temperature to $1 \cdot 10^7\ cm^{-3}$ and about $2 \cdot 10^7\ cm^{-3}$ for engine temperatures of 328 and 355 K, respectively.

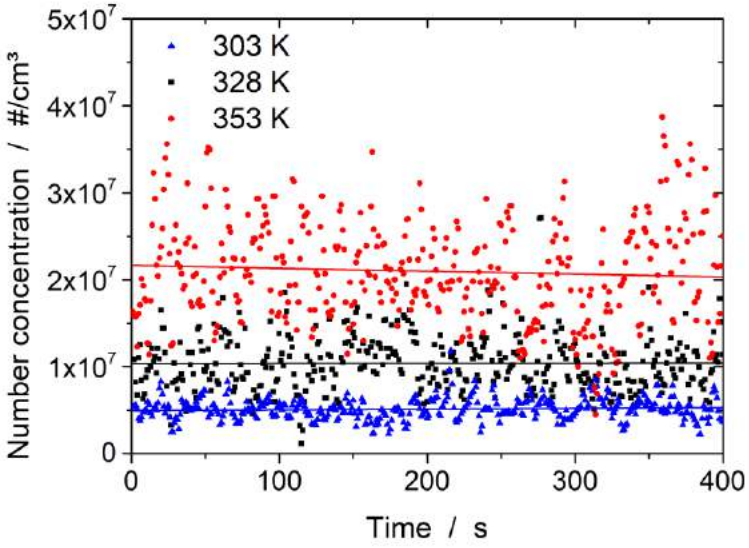

Figure 17: Soot total number concentrations versus the measurement time for three different engine temperatures and iso-octane as fuel.

Since also the SOI were varied within the cases with different engine temperatures, the fuel-film evaporation times for the engine temperatures of 328 and 353 K and an SOI of -360 °CA need to be calculated based on the results from Figure 7. Assuming that in every case the fuel was injected at -360 °CA results in evaporation times of 1, 4 and 4.6 cycles for the temperatures 355, 328 and 303 K, respectively, according to the data from Section 3.1.3. This results in total soot concentrations of $2 \cdot 10^7\ cm^{-3}$, $4 \cdot 10^7\ cm^{-3}$ and $2.3 \cdot 10^7\ cm^{-3}$ for the temperatures of 355, 328 and 303 K. In addition, the injection duration was 2.5 ms for the case with a temperature of 303 K, so that the soot concentration would be even lower if the injection duration was 1.7 ms as in the other cases. However, the different SOI and injection durations make a comparison of the soot concentrations difficult. Measurements on fuel-film evaporation in the wind tunnel have shown that an increase in temperature resulted in an increase in the initial fuel-film mass about 200%, from 0.16 to 0.5 mg. However, the LIF images from the work reported

here are not of quantitative nature, giving information about the fuel-film thickness or mass. Results from the optical engine for these operating points are still in the post processing by BOSCH.

Soot incandescence, integrated over the entire field of view at different crank angles, is shown in Figure 18. In contrast to the soot concentration measured in the exhaust, the soot incandescence is of similar magnitude at engine temperatures of 303 and 328 K. Again, an increase in the engine temperature correlates with an increase in the soot-particle number concentration and also soot incandescence, as shown in Figure 18.

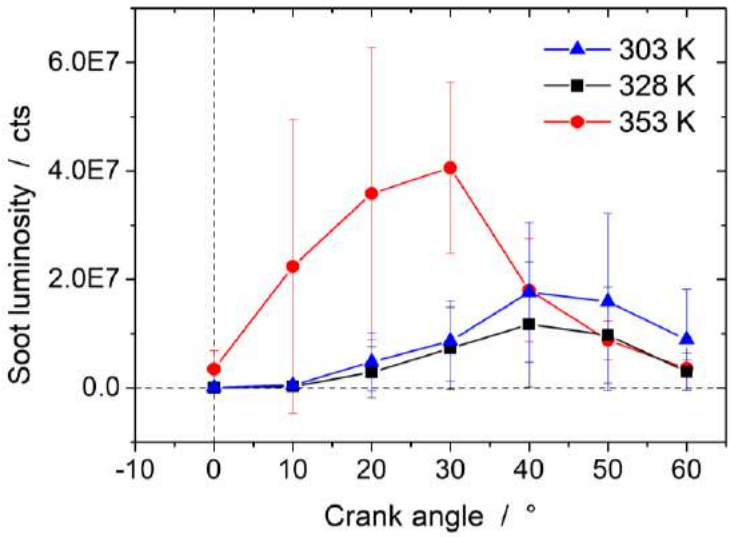

Figure 18: Integrated soot incandescence for three different engine temperatures and iso-octane as fuel. Error bars indicate the standard deviation in the soot incandescence from 10 single cycles.

3.2 Visualization of spray, flame front, and soot incandescence

Figure 19 shows a high-speed real-colour image sequence of the spray at SOI = -320 °CA and P_{inj} = 100 bar. The engine speed was 1200 min^{-1} and T_{eng} was 303 K. Images were taken with 1 °CA resolution, but fewer images are shown here. The delay between the electronic and hydraulic SOI can be observed here, as the injection only starts at -318 °CA instead of -320 °CA. The piston surface is also visible and the wear pattern due to impinging jets can be seen here. Also, oil droplets are visible on the piston surface. The jet impingement areas in the first two images appear to be dry and without droplets, which confirms that the droplets in the other area are actually from engine oil. The fuel-jets were narrow and distinct at the start, but increased in cross-section at later crank angles (-305 °CA and -300 °CA). By this method, jet behaviour at different conditions can be studied under real engine conditions.

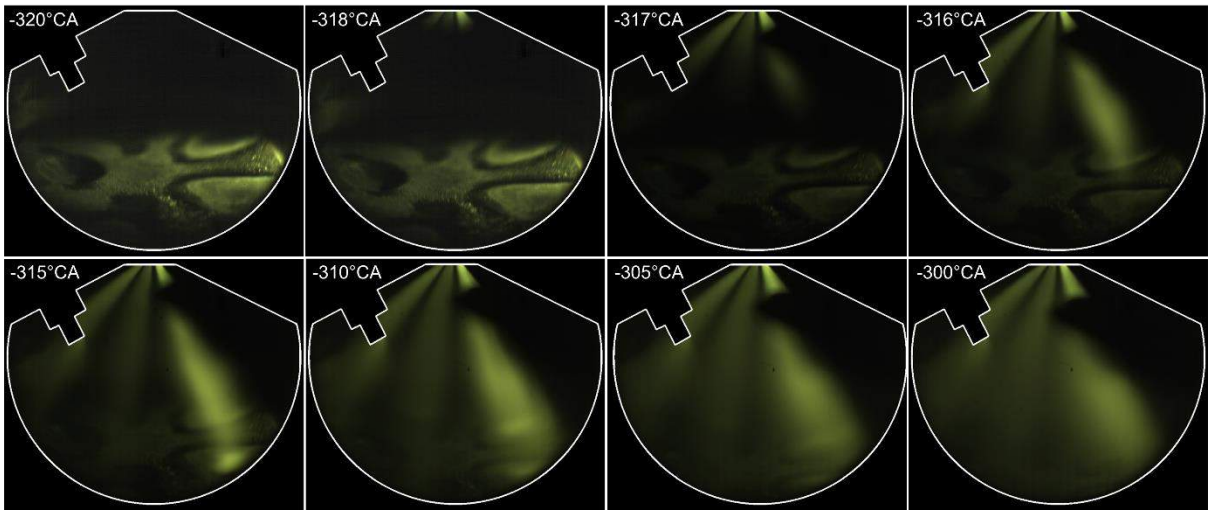

Figure 19: High-speed visualization of spray jets. Fuel: iso-octane/toluene, n = 1200 min^{-1}, T_{eng} = 303 K, SOI at -320 °CA, P_{inj} 100 bar.

Figure 20 shows the high-speed real colour chemiluminescence and soot visualization at the same operating conditions as in measurement shown in Figure 19. The ignition timing was -38 °CA. It can be observed here that the chemiluminescence and soot formation are temporally separated, as already reported in D 1.6. Very weak chemiluminescence signals are visible at -20 °CA, and the flame size increases with time. At 5 °CA, soot starts appearing in the areas of fuel-film. At this crank angle, chemiluminescence is still visible, but is dimmed due to high intensity of soot. In later crank angles, the local soot formation in the regions of fuel-films can be observed. Upon comparing the image -320 °CA (piston at same height) in Figure 19, it becomes evident that the location of soot incandescence was the same as the location of impinging jet/fuel-film. Also, the soot formation appears to be in the form of upward fumes, which is due to simultaneous evaporation of fuel-films and their conversion into soot.

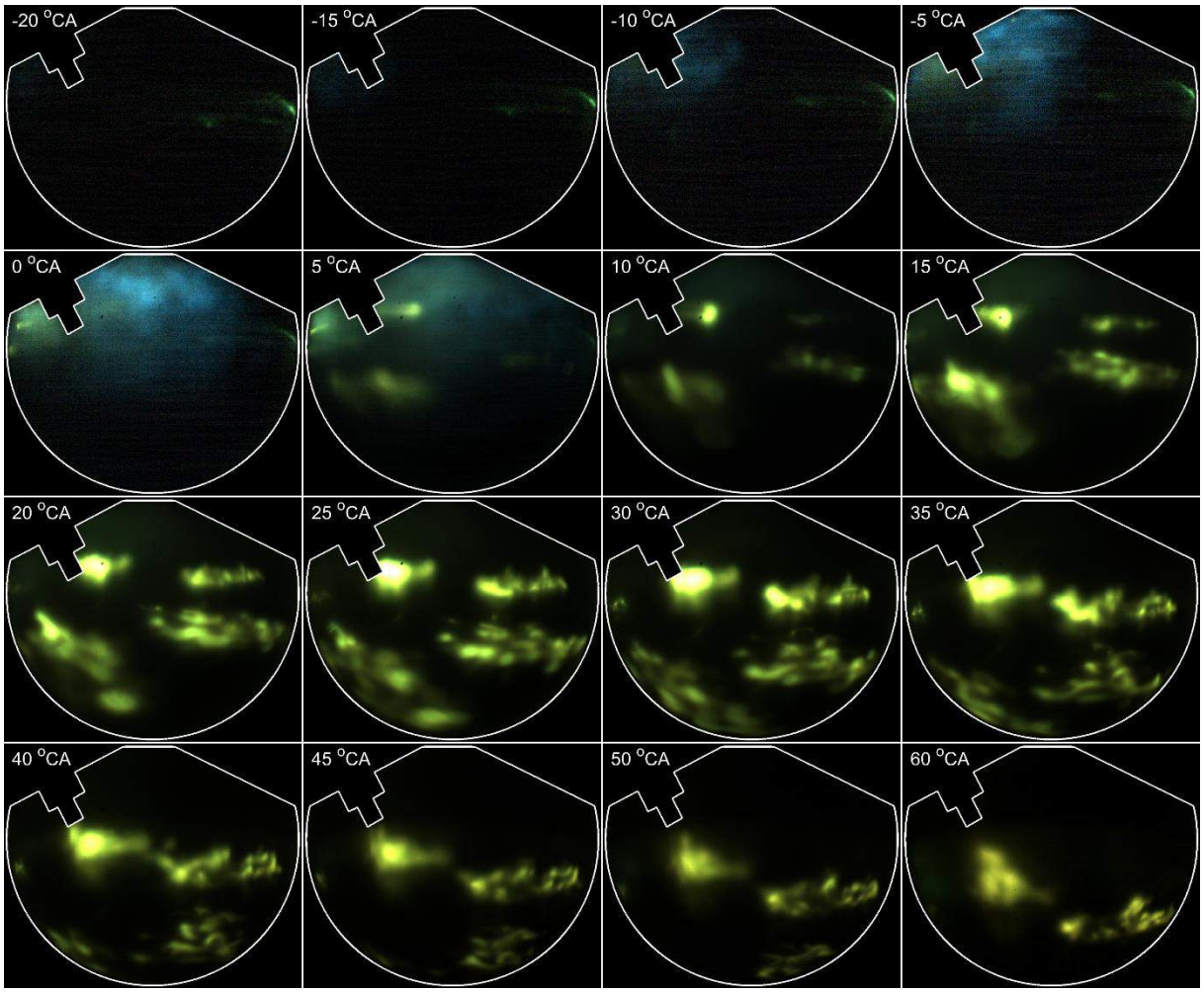

Figure 20: High-speed imaging of blue flame chemiluminescence and yellow-green soot incandescence. The latter appears green because of the blue glass filter in front of the camera lens. Fuel: iso-octane/toluene ,n = 1200 min^{-1}, T_{eng} = 303 K, SOI at -320 °CA, P_{inj} 100 bar, ignition at -38 °CA.

4 Conclusions and implications for combustion strategies

In a joint effort, BOSCH and UDE developed and tested strategies to image fuel-film formation and evaporation as well as on combustion in an endoscopically accessible DISI engine. Gasoline and iso-octane fuel-films were visualized by LIF. First, the evaporation time of fuel-films under motored conditions was investigated for varying injection time, engine temperature and injection pressure. Second, fuel-films and soot were simultaneously visualized via the double-frame feature of an intensified CCD camera with a quick-decay phosphor. Third, high-speed colour combustion-imaging showed the scattered light from the spray, the chemiluminescence of the flame, and soot incandescence.

The results showed that gasoline fuel-films can last for a comparatively long time (several cycles) on the piston surface under cold-start and skip-fire conditions. At an engine temperature of 303 K, the average fuel-film survival time reduced from 28 to 18 cycles when changing the SOI from -360 °CA to -320 °CA. For an engine temperature of 353 K, the fuel-films survive for a similar number of cycles when varying the SOI. Increasing the injection pressure from 100 to 350 bar reduces the fuel-film survival time by about 50%, from 28 to 14 cycles for an engine temperature of 303 K. Also, for an engine temperature of 353 K, the survival time is reduced by about 50%, from 5.5 to 3 cycles. The increase in the engine temperature from 303 K to 353 K reduces the fuel-film lifetime about 77% from 28 to 6.3 cycles, respectively, and has the largest influence on the evaporation time compared to other parameters that were investigated.

In general, iso-octane fuel-films evaporate much faster than gasoline films, due to their lack of low-volatile components. The fuel-film survival time is reduced from 2.3 cycles to 1 cycle at an engine temperature of 303 K, and from 1 to 0.5 cycles for an engine temperature of 353 K when changing the SOI from -320 to -360 °CA. An increase in the injection pressure from 100 to 350 bar reduces the lifetime from 2.3 to 1.6 cycles at a temperature of 303 K and from 1 to 0.5 cycles for a temperature of 353 K. Again, the engine temperature has the largest influence on film lifetime. Raising the temperature from 303 to 353 K reduces the lifetime by about 65%, from 2.3 cycles to 1 cycle.

The fuel-film evaporation characteristics show that, in particular under cold start conditions, it is important to set the SOI to later crank angles with respect to gas exchange TDC. Increasing the injection pressure can also help reducing the lifetime of fuel-films under cold-start conditions. For both fuels, combustion has no significant influence on the film lifetime. This is in good agreement with previous results on fuel-film evaporation in the flow channel at UDE reported in D1.6 and [11].

Simultaneous visualization of the fuel-film and soot (the latter via incandescence) shows the individual fuel-films on the piston surface and soot incandescence in abutting regions. While at an engine temperature of 303 K, the gasoline fuel-films 5 and 6 appear as independent isolated spots, at 353 K they merge to a contiguous film with spatially varying thickness. Most probably, the decreasing viscosity of both fuel and oil, which has accumulated on the piston surface, leads to this phenomenon. While very little soot is seen in the colder case, a high intensity of soot incandescence is detected in the hot case. However, the long lifetime of the fuel-films under cold conditions results in soot formation over many more cycles. Taking the longer lifetime of fuel-films under cold conditions into account, in terms of correcting the evaporation times about the varied parameters, results in particle concentrations of $3.8 \cdot 10^{8}\ cm^{-3}$ and $8.5 \cdot 10^{7}\ cm^{-3}$ for engine temperatures of 353 and 303 K, respectively. The high soot-particle concentration for an engine temperature of 353 K stems from the accumulation of oil on the piston surface in the experiments with gasoline. For the visualization of iso-octane fuel-films and soot, the engine was fuelled with methane before every measurement to clean the piston from remaining oil. However, for a

stable engine operation, the SOI and the injection duration needed to be optimized throughout the measurements with increasing engine temperature and iso-octane.

High-speed colour imaging showed spray and combustion propagation in real time. The delay between electronic and hydraulic SOI was observed to be 2 °CA (277.8 µs). Also, the variation in plume cone angle at different conditions could be visualized. The high-speed combustion imaging showed that chemiluminescence is temporally separated from soot formation, with the latter starting around 20 to 20 °CA afterwards. It was also observed that soot formation started primarily in the regions of the fuel-films.

The implications of current findings for the combustion strategies are summarized below in Table 3.

Table 3: Effect of investigated parameters on fuel-film survival time and soot number concentration.

Parameters	Fuel-film survival time	Soot-particle number concentration
Increase in **injection pressure** (Pinj)	**Decreases**. Effect more pronounced for gasoline than for iso-octane. The fuel-film survival time decreased about 30% to 50 % when increasing Pinj from 100 to 350 bar.	not investigated
Later **start of injection** (SOI)	**Decreases.** Effect more pronounced for lower Teng and similar for either fuels. Decrease in survival time about 36% to 56% for Teng = 303 K.	not investigated
Increase in **engine temperature** (Teng)	**Decreases.** Most significant parameter for fuel-film survival time. Decrease in fuel-film survival about 60% when Teng increased from 303 K to 328 K.	**Increases.** Higher fractions of fuel-films evaporate within one cycle at higher Teng, and contribute to soot formation. The effect of continuous combustion is not investigated. Soot-particle number concentration is expected to be higher for cold conditions under continuous-fire mode.

5 Risk Register

Risk No.	What is the risk	Probability of risk occurrence[1]	Effect of risk[2]	Solutions to overcome the risk
1	Transferability of insights from skip-fired operation to a continuously fired, real engine	2	2	Take the impact of continuously fired operation compared to skip-fired operation in the analysis of the results into account.
2	Oil on the piston surface, significantly contributing to soot formation.	1	2	Fuel the engine with methane until measured soot-particle number concentrations is below a threshold before starting the next measurement.
3	Oil in the fuel-films region, emitting LIF signal after illumination which interfered with fuel-film LIF signal => impact on predicted fuel-film evaporation times.	1	2	Fuel the engine with methane until measured soot-particle number concentrations is below a threshold before starting the next measurement.
4	Some cooling water could have entered into the engine oil while cleaning the illumination endoscope.	3	2	Tighten the illumination endoscope with a torque wrench and inspect the combustion chamber through spark-plug hole with a borescope before measurements.

[1] Probability risk will occur: 1 = high, 2 = medium, 3 = Low

[2] Effect when risk occurs: 1 = high, 2 = medium, 3 = Low

Appendix A – Acknowledgement

The author(s) would like to thank the partners in the project for their valuable comments on previous drafts and for performing the review.

Project partners:

#	Partner	Partner Full Name
1	RIC	RICARDO UK LIMITED
2	DAI	DAIMLER AG
3	JLR	JAGUAR LAND ROVER LIMITED
4	BOSCH	ROBERT BOSCH GMBH
5	FEV	FEV EUROPE GMBH
6	JM	JOHNSON MATTHEY PLC
7	HON	HONEYWELL, SPOL. S.R.O
8	JRC	JOINT RESEARCH CENTRE – EUROPEAN COMMISSION
9	UNR	UNIRESEARCH BV
10	IDIADA	IDIADA AUTOMOTIVE TECHNOLOGY SA
11	SIEMENS	SIEMENS INDUSTRY SOFTWARE SAS
12	LOGE	LUND COMBUSTION ENGINEERING LOGE AB
13	ETH	EIDGENOESSISCHE TECHNISCHE HOCHSCHULE ZUERICH
14	UDE	UNIVERSITAET DUISBURG-ESSEN
15	RWTH	RWTH AACHEN UNIVERSITY
16	UFI	UFI FILTERS SPA
17	UOB	UNIVERSITY OF BRIGHTON
18	Garrett	GARRETT MOTION CZECH REPUBLIC SRO

This project has received funding from the European Union's Horizon2020 research and innovation programme under Grant Agreement no. 723954.

6 References

1. Warey, A., Huang, Y., D. Matthews, R., Hall, M., and Ng, H., "Effects of Piston Wetting on Size and Mass of Particulate Matter Emissions in a DISI Engine," SAE Technical Paper 2002-01-1140, 2002, doi:10.4271/2002-01-1140.
2. Drake, M.C., Fansler, T.D., Solomon, A.S., and Szekely, G., "Piston fuel films as a source of smoke and hydrocarbon emissions from a wall-controlled spark-ignited direct-injection engine," SAE Technical Paper 2003-01-0547, 2003, doi:10.4271/2003-01-0547.
3. Ortmann, R., Arndt, S., Raimann, J., Grzeszik, R., and Würfel, G., "Methods and Analysis of Fuel Injection, Mixture Preparation and Charge Stratification in Different Direct Injected SI Engines," SAE Technical Paper 2001-01-0970, 2001, doi:10.4271/2001-01-0970.
4. Stevens, E., and Steeper, R., "Piston Wetting in an Optical DISI Engine: Fuel Films, Pool Fires, and Soot Generation," SAE Technical Paper 2001-01-1203, 2001, doi:10.4271/2001-01-1203.
5. Stojkovic, B.D., Fansler, T.D., Drake, M.C., and Sick, V., "High-speed imaging of OH* and soot temperature and concentration in a stratified-charge direct-injection gasoline engine," *Proceedings of the Combustion Institute* 30(2):2657-2665, 2005, doi:10.1016/j.proci.2004.08.021.
6. Li, J., Matthews, R.D., Stanglmaier, R.H., Roberts, C.E., and Anderson, R.W., "Further Experiments on the Effects of In-Cylinder Wall Wetting on HC Emissions from Direct Injection Gasoline Engines," SAE Technical Paper 1999-01-3661, 1999, doi:10.4271/1999-01-3661.
7. H. Stanglmaier, R., Li, J., and D. Matthews, R., "The Effect of In-Cylinder Wall Wetting Location on the HC Emissions from SI Engines," SAE Technical Paper 1999-01-0502, 1999, doi:10.4271/1999-01-0502.
8. Li, J., Huang, Y., Alger, T., et al., "Liquid Fuel Impingement on In-Cylinder Surfaces as a Source of Hydrocarbon Emissions From Direct Injection Gasoline Engines," *Journal of Engineering for Gas Turbines and Power* 123(3):659-668, 2001, doi:10.1115/1.1370398.
9. Alger, T., Huang, Y., Hall, M., and Matthews, R.D., "Liquid Film Evaporation Off the Piston of a Direct Injection Gasoline Engine," SAE Technical Paper 2001-01-1204, 2001, doi:10.4271/2001-01-1204.
10. Schulz, F., and Beyrau, F., "Systematic Investigation of Fuel Film Evaporation," SAE Technical Paper 2018-01-0310, 2018, doi:10.4271/2018-01-0310.
11. Jüngst, N., and Kaiser, S., "Imaging of Fuel-Film Evaporation and Combustion in a Direct-Injection Model Experiment," SAE Technical Paper 2019-01-0293, 2019, doi:10.4271/2019-01-0293.
12. Geiler, J.N., Grzeszik, R., Quaing, S., Manz, A., and Kaiser, S.A., "Development of laser-induced fluorescence to quantify in-cylinder fuel wall films," *International Journal of Engine Research* 19(33):134-147, 2018, doi:10.1177/1468087417733865.
13. Gessenhardt, C., Schulz, C., and Kaiser, S.A., "Endoscopic temperature imaging in a four-cylinder IC engine via two-color toluene fluorescence," *Proceedings of the Combustion Institute* 35(3):3697-3705, 2015, doi:10.1016/j.proci.2014.06.085.
14. Goschütz, M., Schulz, C., and Kaiser, S.A., "Endoscopic Imaging of Early Flame Propagation in a Near-Production Engine," *SAE International Journal of Engines* 7(1):351-351, 2014, doi:10.4271/2014-01-1178.
15. Geiler, J.N., "Bildgebende Messung der Kraftstoffwandfilmdicke durch laserinduzierte Fluoreszenz," University of Duisburg-Essen, 2019.